JMEPEG (2011) 20:641–645
DOI: 10.1007/s11665-011-9845-z

1059-9495/$19.00

An Evaluation of a NiTiCo Alloy and its Suitability for Medical Device Applications

Audrey Fasching, D. Norwich, T. Geiser, and Graeme W. Paul

(Submitted June 17, 2010; in revised form September 17, 2010)

Development of a superelastic material with higher stiffness and plateau stresses than binary nitinol is of interest to the medical device industry because it may allow for lower profile, less intrusive devices without compromising the material's characteristics. This project studied the effect of cobalt (Co) alloying additions on the stiffness and plateau stresses of a superelastic nickel-titanium alloy. In addition, the general physical, mechanical, corrosion, and biocompatibility properties of the alloy were compared to binary nitinol. The results of this study showed Co to be an interesting alloying addition that should be considered for future medical devices in applications, where stiffness is of concern.

Keywords biocompatibility, corrosion, high-stiffness nitinol, NiTiCo, nitinol, strain-life curves, superelastic

1. Introduction

Ternary alloy formulations are not new for nitinol alloys, the dental industry was interested in NiTiCo alloys 35 years ago (Ref 1). Several researchers studied the effect of alloying additions which include: gold (Au), palladium (Pd), cobalt (Co), manganese (Mn), and zirconium (Zr) (Ref 2). The transformation and mechanical properties of Ni-Ti-Co alloys have also been examined (Ref 2, 3). Hosoda et al. and Kishi et al. showed that Co additions increase the yield strength and decrease the M_s of the alloys. In alloys with ternary additions of Co, it is believed that Co occupies Ni lattice sites. Co is well accepted as an implantable element and as such is the focus of this investigation.

An on-going alloy development program at SAES Smart Materials (SSM) resulted in the creation of a family of superelastic alloys with increased modulus (i.e., high-stiffness nitinol). One of these new alloys contained minor Co additions. The purpose of this project was to compare basic mechanical and physical properties between a standard body temperature binary NiTi alloy and a ternary NiTiCo alloy. The scope of this study was to collect data useful for medical device applications.

This article is an invited paper selected from presentations at Shape Memory and Superelastic Technologies 2010, held May 16-20, 2010, in Pacific Grove, California, and has been expanded from the original presentation.

Audrey Fasching, D. Norwich, and **T. Geiser**, SAES Memry Corporation, Bethel, CT; and **Graeme W. Paul**, SAES Smart Materials, New Hartford, NY. Contact e-mail: audrey_fasching@memry.com.

2. Experimental Procedure

A NiTiCo ingot was fabricated at SAES Smart Materials with a chemical composition consistent with ASTM F 2063-05 for standard binary nitinol with the exception of Co content. Co additions range between 1 and 2 at.% for this alloy. All of the samples for this study were produced from one lot of 1.3 mm (0.052 in.) diameter wire that was cold worked and drawn to a final diameter of 0.381 mm (0.015 in.). Where comparisons are made between the NiTiCo alloy and binary nitinol, Nitinol Alloy BB (50.8 at.% Ni) was used.

Inclusion analysis was conducted in accordance with ASTM F 2063-05. Samples were not available in the mill product as specified by ASTM F 2063-05; so the measurements were made on sections of 2.67 mm (0.105 in.) diameter and compared to similar size binary NiTi. Differential scanning calorimeter (DSC) tests were conducted on cold-worked and shape-set parts per ASTM F 2004-03 to determine transformation temperature with an Instrument Specialists DSC 550.

The bending modulus was measured via three-point bend test using a MTS SinTech test apparatus with an 8.9 kN load cell. The SinTech system used knife edges and a gap distance of 20.6 mm (0.810 in.). Tests were conducted at room temperature using 1.02 mm (0.040 in.) diameter wire. Samples were bent to a maximum deflection of 4.06 mm (0.16 in.) at a rate of 2.54 mm/min (0.10 in./min). The data was fit to a straight line by linear regression and the bending modulus was determined. Data for both binary NiTi and NiTiCo fit a straight line very well having R^2 values of 0.986 and 0.992, respectively.

Shape-set, straight 0.381-mm diameter wire samples were used for both tensile and fatigue testing. All heat treatments were conducted in a salt pot; the actual times and temperatures are proprietary to SAES Memry and, as such, are not reported here. The heat-treatment parameters were optimized for the NiTiCo alloy and are different from the standard binary alloy. Active Af was measured by bend-free recovery (BFR) per ASTM F 2082-06 and is reported, for each alloy, in Table 1.

Tensile tests were conducted on an Instron 5565 load frame with a 5 kN load cell as per ASTM F 2516-05. Tensile tests to failure (TTF) and 6% strain tests were performed on straight,

shape-set wire samples. Ten samples were tested and averaged for the final results. Ten-cycle load/unload tensile tests were loaded to 6% strain and unloaded with all other test parameters per ASTM F 2516-05. All testing was conducted at room temperature using an Epsilon 3442-0050-010 ST clip-on extensometer.

Fatigue testing was conducted using a rotating beam fatigue tester (RBT) with a zero mean, 0.8% maximum alternating strain. The samples were rotated at a constant speed and guided in a test block machined with a radius to provide the desired level of strain. The fixture can test up to 10 samples at a time and counts revolutions on each sample individually using a laser counter. The RBT test is designed to provide comparative results for materials processed with different parameters at the same or varying strain levels. Tests were performed in a circulating 37 °C water bath at 1000 rpm to eliminate any heating effect created in the specimen due to dissipative processes during cyclic loading (cyclic stress-induced formation and reversion of martensite). The heat transfer from the specimen to the test environment helps to counteract this process.

Fatigue curves showing strain versus number of cycles to failure (Strain-*N*) were generated for etched and electropolished wire and tested with the rotating beam tester described above. Test blocks were made to provide strains of 2.3, 1.8, 1.0, 0.8, and 0.65%. Three samples of each wire size were tested at each strain level. The test was run to failure or suspended at 10 million cycles.

Potentiodynamic polarization tests were performed on electropolished wire samples in accordance with ASTM F 2129-05. The rest potential (E_r) was monitored for 1 h after immersion of each sample, and the potentiodynamic scan was then performed at a rate of 1.0 mV/s. In each case, the potential scan was started from E_r and, if breakdown did not occur, was continued up to a vertex potential (E_v) of approximately 0.8 V (SCE). The polarization tests were performed using a computer-controlled electrochemical testing system (Gamry Instruments). All potentials were measured with respect to a saturated calomel electrode (SCE). A graphite rod was used as a counter electrode for the polarization tests.

Two representative biocompatibility tests were run to determine if the presence of Co would affect the overall biocompatibility of the NiTiCo alloy. Two basic tests were selected and sent to an outside laboratory for analysis. The first test, cytotoxicity (ISO 10993-5), is known for being a rapid, standardized test that is sensitive and inexpensive. The results determine whether a sample contains significant quantities of harmful extractables (i.e., Ni, Co) and what their effect may have on cellular components. The second test, hemolysis (ASTM F756-08), determines compatibility of devices designed for direct or indirect contact with circulating blood. Effectively, hemolysis measures the ability of a material to cause red blood cells to rupture. Electropolished 0.533 mm (0.021 in.) diameter NiTiCo and binary NiTi wire were evaluated for biocompatibility.

Table 1 Summary of ingot properties of binary NiTi and NiTiCo

Property	Binary NiTi	NiTiCo
As (fully annealed ingot), °C	−15	−80
Af (DSC), °C	+5 ± 10	−67
Af (BFR), °C, straight annealed wire	7	11
Maximum inclusion length, μm	19.77	11.34
Maximum inclusion area fraction, %	0.97	0.71

3. Results and Discussion

Basic transformation and inclusion properties were measured on the NiTiCo alloy and are compared to binary NiTi in Table 1. As stated previously, Co additions have been shown to lower the transition temperature of nitinol alloys. NiTiCo alloys with warmer transition temperatures are also in development but will not be discussed in this study. Transition temperature was measured on the ingots using DSC and then again on the final wire product using bend and free recovery (BFR) per ASTM F 2082-06. While the austenite transition temperatures in the ingot varied by approximately 60 °C; after manufacturing and final processing with optimized heat treatments, the Af of both NiTiCo (11 °C) and binary NiTi (7 °C) were similar. The maximum inclusion size and area fraction measured in the longitudinal direction for the NiTiCo alloy were well within ASTM F 2063-05. Typical results for a binary NiTi alloy at the redraw stage are also reported. For this particular ingot, the NiTiCo alloy exhibited significantly smaller maximum inclusion size than the binary alloy; however, it is not uncommon to observe a binary alloy with a maximum inclusion size in a range similar to the NiTiCo alloy examined in this study.

Average tensile data for each alloy is summarized in Table 2. Active Af was measured on wires with optimized heat treatments for both binary NiTi (7 °C) and NiTiCo (11 °C). The active Af of both alloys was close and allowed for a reasonable comparison of the mechanical properties. Exemplar stress-strain curves for binary NiTi and NiTiCo are shown in Fig. 1 and 2 respectively. Similar ultimate tensile strength was observed for both NiTiCo and binary NiTi. The upper and lower plateau increased significantly in the NiTiCo alloy compared to binary; however, the difference between the upper and lower plateau was the same for both alloys (~269 MPa). The upper (710 MPa) and lower (439 MPa) plateau values for the NiTiCo alloy are approximately 30% higher than for the binary alloy. These results agree with the bending modulus data; where modulus of NiTiCo was found to be 586 MPa compared to 414 MPa for the binary NiTi alloy, this represents nearly a 30% higher modulus for the NiTiCo alloy.

Table 2 Mechanical property comparison of binary NiTi and NiTiCo

Property	Binary NiTi	NiTiCo
Loading plateau stress @ 3% strain, in austenite	492 MPa (71.3 ksi)	710 MPa (103 ksi)
Unloading plateau stress @ 3% strain, in austenite	226 MPa (32.8 ksi)	439 MPa (63.7 ksi)
UTS in austenite	1320 MPa (191 ksi)	1320 MPa (191 ksi)
Max. residual elongation after 6% strain in austenite	0.1	0.3
Bending modulus (three-point bend)	414 MPa (60 ksi)	586 MPa (85 ksi)

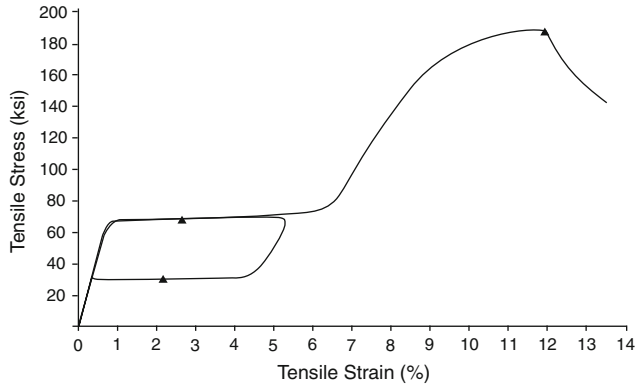

Fig. 1 Typical stress-strain curve for binary nitinol alloys

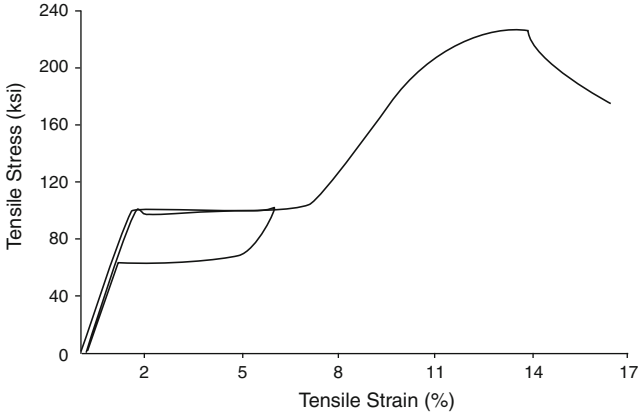

Fig. 2 Typical stress-strain curve for high-stiffness NiTiCo alloys

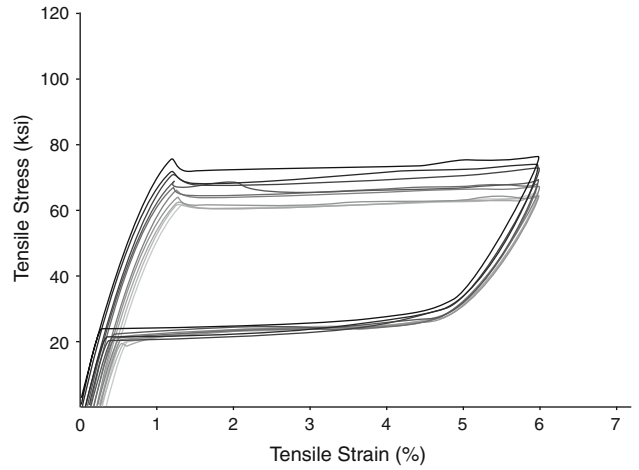

Fig. 3 Ten-cycle load/unload curve for binary nitinol, only minor ratcheting apparent

The tensile data also indicated that NiTiCo had more residual strain than the binary alloy; further investigation was conducted to determine the effect of multiple cycles on the tensile properties. Ten-cycle load/unload curves, shown in Fig. 3 and 4, examined the change in hysteresis loop over several cycles. A lowering of the upper plateau and an increase in permanent set with cycling were observed for both alloys.

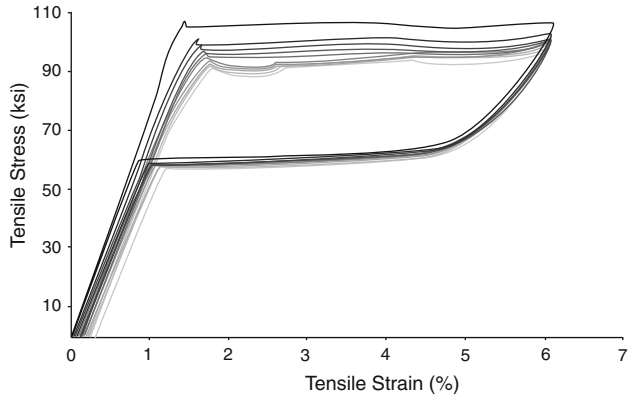

Fig. 4 Ten-cycle load/unload curve for NiTiCo, exhibits some ratcheting

Table 3 Tabulated fatigue data for 0.015 in. diameter wire; samples were tested to failure or 10 million cycles

Stress, %	Number of cycles to failure binary NiTi	Number of cycles to failure NiTiCo
2.34	957	750
2.34	1307	775
2.34	1193	795
1.77	3048	1150
1.77	3286	1190
1.77	3274	1100
1.00	9931	7550
1.00	9578	7600
1.00	9465	8150
0.80	14,650	15,849
0.80	19,834	12,444
0.80	19,160	19,690
0.65	10,000,000	10,000,000
0.65	10,000,000	10,000,000
0.65	10,000,000	10,000,000

A full 6% strain was still achievable for both alloys after 10 cycles. Total residual strain or permanent set was similar for both NiTiCo and binary NiTi after 10 cycles.

The fatigue data is tabulated in Table 3 and plotted in Fig. 5. The data represents three samples per strain level and five strain conditions; all data points are plotted in the Strain-*N* graph (Fig. 5). NiTiCo showed a decrease in fatigue life compared to NiTi when tested in low cycle strain control. At high cycles there was no difference between the alloys, and both showed evidence of an endurance limit. The decreased low cycle fatigue can be attributed to a higher upper plateau exhibited by the NiTiCo alloy as compared to the binary NiTi alloy. For a given strain, the stress will be lower in the alloy with the lower plateau (NiTi) than the alloy with the higher plateau (NiTiCo). The lines converge at higher cycles because the strain levels are low enough to remain in the linear elastic region for both alloys.

Cyclic polarization scans were performed on electropolished and passivated wire samples to determine the pitting corrosion performance of the wire. An example of the polarization results for NiTiCo is shown in Fig. 6. No breakdown was observed in any of the NiTiCo. No breakdown means the sample did not exhibit pitting corrosion during the test cycle; this corresponds

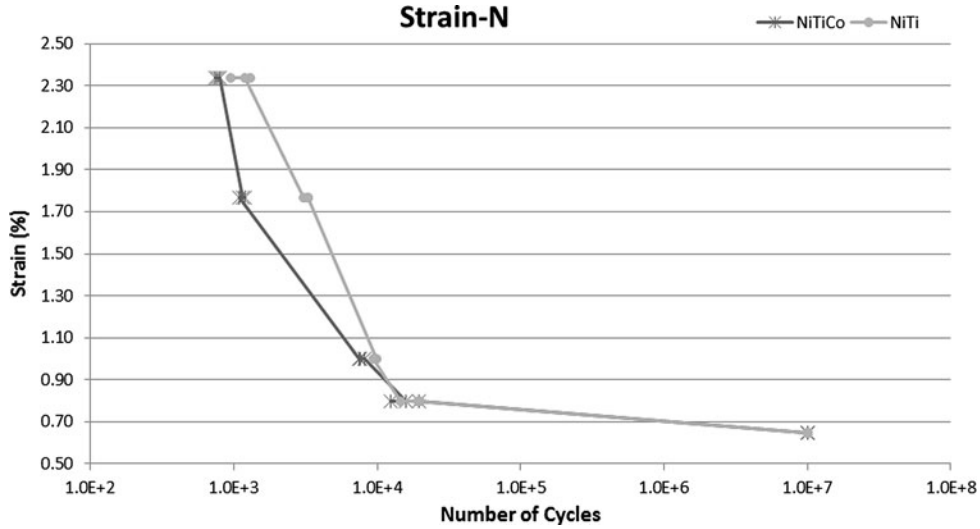

Fig. 5 Strain vs. number of cycles to failure comparing NiTiCo to binary NiTi

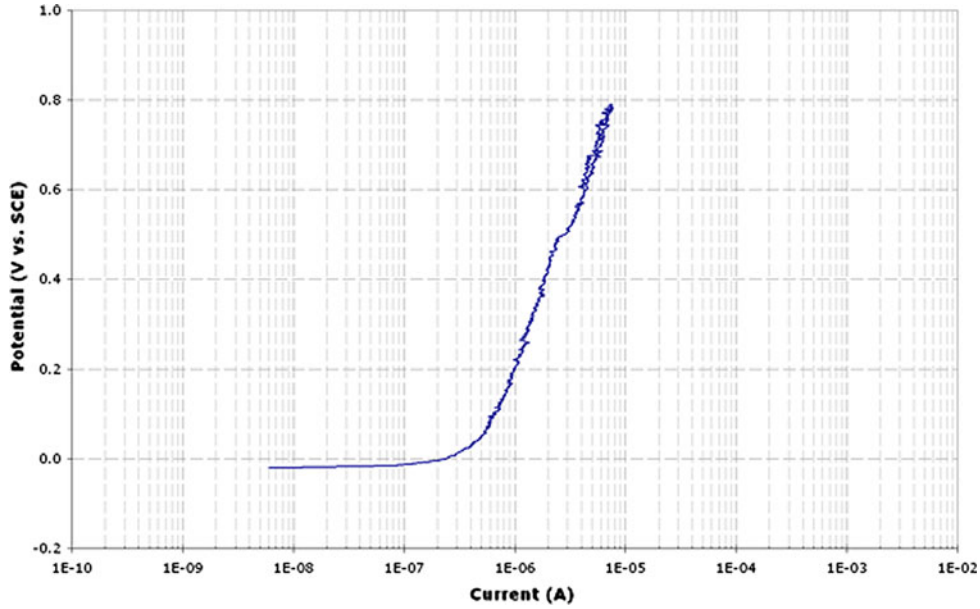

Fig. 6 Cyclic potentiodynamic polarization data for NiTiCo showing no breakdown

to a high level of corrosion resistance. Similar electropolished and passivated binary NiTi wire also did not breakdown during the ASTM F 2129-05 tests.

Cytotoxicity is the quality of being toxic to cells. Cytotoxicity testing was performed using the MEM elution method to evaluate the toxicity or irritancy potential of the material. In addition to the NiTiCo samples, NiTi material was also submitted to act as a baseline reference. Both the binary nitinol and NiTiCo wires scored zero, or no reactivity according to the qualitative evaluation of the cells exposed to the extracts. ISO specifications state that a numerical grade of 2 or greater is considered to have a cytotoxic effect.

Hemolysis determines compatibility of devices designed for direct or indirect contact with circulating blood. The test measures the ability of a material to cause red blood cells to rupture. The hemolytic grades for the test article and positive control are assigned by ASTM F 756-08. The corrected hemolytic index for the binary nitinol and NiTiCo test articles was zero. Therefore, the test article is considered non-hemolytic by the direct contact method according to the hemolytic grading criteria in the ASTM F 756-08 standard.

4. Conclusions

- NiTiCo alloy has approximately a 30% higher modulus, loading plateau and unloading plateau when compared to the binary alloy.

- Fatigue tests resulted in similar strain-life curves to binary NiTi, when tested in strain controlled, zero mean strain rotating beam testing.
- Electropolished and passivated NiTiCo wire did not exhibit breakdown when subjected to potentiodynamic polarization testing as per ASTM F 2129-05. NiTiCo has similar corrosion resistance to binary NiTi.
- Biocompatibility performance is similar between NiTi and NiTiCo and exhibited no reactivity in both the cytotoxicity and hemolysis tests performed in this study.

References

1. S. Civjan, E.F. Huget, and L.B. DeSimon, Potential Applications of Certain Nickel-Titanium (Nitinol) Alloys, *J. Dent. Res.*, 1975, **54**, p 89–96
2. H. Hosoda, S. Handada, K. Inoue, T. Fukui, Y. Mishima, and T. Suzuki, Martensite Transformation Temperatures and Mechanical Properties of Ternary NiTi Alloys With Off Stoichiometric Compositions, *Intermetallics*, 1998, **6**, p 291–301
3. Y. Kishi, Z. Yajima, and K. Shimizu, Relation Between Tensile Deformation Behavior and Microstructure in a Ti-Ni-Co Shape Memory Alloy, *Mater. Trans.*, 2002, **43**(5), p 834–839